Sc-doped barium hexaferrite nanodiscs: Tuning morphology and magnetic properties

Martin Hähsler[a,b], Michael Zimmermann[a], Stefan Heißler[c], Silke Behrens[a,b,*]

[a] Institute of Catalysis Research and Technology, Karlsruhe Institute of Technology, Postfach 3640, 76021 Karlsruhe, Germany
[b] Institute of Inorganic Chemistry, Ruprecht-Karls University Heidelberg, Im Neuenheimer Feld 270, 69120 Heidelberg, Germany
[c] Institute of Functional Interfaces, Karlsruhe Institute of Technology, Postfach 3640, 76021 Karlsruhe, Germany

ARTICLE INFO

Keywords:
Magnetic nanodiscs
Barium hexaferrite
Hydrothermal synthesis
Hard ferrites

1. Introduction

Magnetic nanoparticles exhibit size- and shape-dependent magnetic properties [1,2] and have attracted great interest for a variety of applications, including catalysis [3,4], magneto-optics [5,6] or magnetic separation of enantiomers [7]. The synthesis and application of nanoparticles consisting of various magnetic materials have been reported, including ferrites (in particular spinel-type ferrites, e.g. Fe_3O_4, $CoFe_2O_4$), metals (e.g. Co, Fe) and alloys (e.g. FePt) while the synthesis of defined nanosized particles of the hexaferrites has remained scarce [8–11]. Hexaferrites possess a hexagonal crystal structure with close packing of oxygen ion layers. Trivalent metal cations are located in interstitial sites of the structure while the heavy ions (e.g. Ba^{2+}) enter substitutionally the oxygen layers. Several types are known depending on their chemical and crystalline structure. Hexagonal ferrites of the M-type such as $BaFe_{12}O_{19}$, are of enormous technical importance, e.g. as permanent magnets due to their low cost, hard magnetic properties and stability in air [12,13]. Bulk $BaFe_{12}O_{19}$ exhibits a saturation magnetization M_s of 72 Am^2/kg at room temperature [12] together with a relatively high magnetocrystalline anisotropy (i.e. anisotropic constant 33×10^4 J/m^3) [14] and a Curie temperature T_c of 740 K [12].

The synthesis of $BaFe_{12}O_{19}$ particles with anisotropic morphology and narrow size distribution has remained challenging [15–17]. As a consequence of very small particle sizes (<10 nm) and poor crystallinity, the magnetic properties of these particles are often rather poor. Barium hexaferrite nanodiscs were obtained in a two-step procedure, where spherical γ-Fe_2O_3 particles were initially prepared and then reacted with BaOH in hydrothermal conditions [18]. The as-obtained discs, however, were rather polydisperse in size and shape. More homogeneous barium hexaferrite nanodiscs with lateral dimensions below 100 nm were obtained directly from barium and iron nitrate precursors in presence of trivalent cation dopants *via* hydrothermal synthesis. Substitution of Fe^{3+} by larger, trivalent cations M^{3+} (i.e. In^{3+}, Sc^{3+}) modified the crystallization kinetics so that $BaFe_{12-x}M_xO_{19}$ with platelet-like morphology and narrow size distribution were obtained *via* hydrothermal synthesis even though no additional ligands were employed. The substitution by smaller cations (i.e. Cr^{3+}) had no influence on particle growth. In general, a higher reaction temperature led to larger particles with higher crystallinity together with an increase in $M_{0.8T}$ and coercivity H_c for all the compositions studied. However, the molar Ba/Sc precursor ratio was restricted to 10:1–2:1 and temperatures of T = 160 °C/240 °C [19]. No further increase in Sc^{3+} dopant and temperatures above 240 °C have been addressed although further improvements, e.g. in the magnetic properties or more narrow size distributions may be expected.

In this study, we systematically address the influence of both the further increase in scandium dopant for a molar Ba/Sc precursor ratio of 1:1 and 1:2, respectively, and the reaction temperature (T > 160–310 °C) on size/shape and magnetic properties during the formation of Sc-doped hexaferrite nanodiscs. The Sc-doped nanodiscs were characterized *via* scanning electron microscopy (SEM), transmission electron microscopy (TEM) and X-ray powder diffraction (XRD). Here, we characterized the nanodisc also *via* IR spectroscopy (IR), Raman spectroscopy and inductively coupled plasma – optical emission spectroscopy (ICP-OES). The magnetization and H_c were determined at room temperature by using an alternating gradient magnetometer

* Corresponding author.
E-mail address: silke.behrens@kit.edu (S. Behrens).

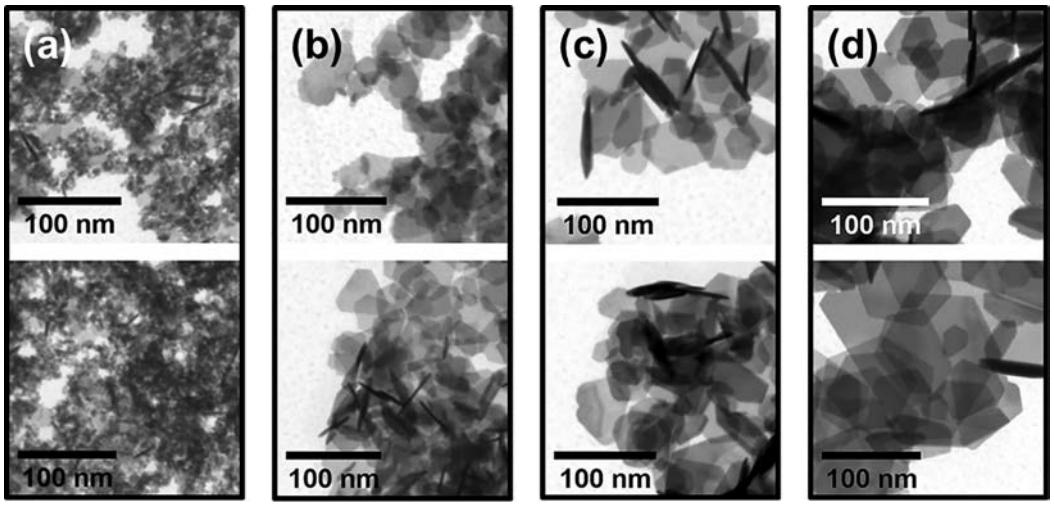

Fig. 1. (a)-(d) SEM micrographs of Sc-doped barium hexaferrite nanodiscs obtained at different reaction temperatures: (a) 160 °C, (b) 210 °C, (c) 260 °C and (d) 310 °C (Ba^{2+}/Sc^{3+}-ratio = 1:1 upper images; 1:2: lower images).

(AGM). This allowed us to establish the correlation between the reaction conditions (i.e. scandium dopant and temperature) and the magnetic properties (e.g. $M_{0.4T}$ and H_c).

2. Experimental

Hydrothermal synthesis of nanodiscs: $Ba(NO_3)_2$ (109 mg), $Fe(NO_3)_3{\cdot}9H_2O$ (molar Ba/Sc precursor ratio 1:1; 758 mg, molar Ba/Sc precursor ratio 1:2; 673 mg) and $Sc(NO_3)_3{\cdot}H_2O$ (molar Ba/Sc precursor ratio 1:1; 85.7 mg, molar Ba/Sc precursor ratio 1:2, 171 mg) were dissolved in distillated H_2O (40 mL). The solution was transferred to an autoclave reactor (100 mL, stainless steel-inlet) loaded with NaOH (4.53 g). The autoclave was closed, vigorously mixed for 10 min, transferred into an oven and heated to the target temperature (heating rate 4 °C/min; T 160 °C, 210 °C, 260 °C, 310 °C). The autoclave was equipped with a thermocouple so that temperature could be measured inside the autoclave. After reaching the target temperature, the autoclave was immediately cooled in air. The crude product was collected *via* centrifugation (5 min, 4000 rcf) and successively washed with 10% HNO_3, 10% acetic acid and acetone. After drying at 80 °C, the nanodiscs were received as a red-brownish solid. The yield of the obtained nanodiscs was dependent on the synthesis conditions and 80 mg (160 °C), 130 mg (210 °C), 175 mg (240 °C), and 175 mg (310 °C), accordingly.

Characterization: The size and the morphology of the nanodiscs were analyzed by SEM using a Zeiss GeminiSEM500 equipped with a Schottky-type field emission cathode. For SEM analysis, the the nanodiscs were suspended in distillated H_2O and deposited on a carbon-coated 400 mesh Cu grid. The maximum diameter (i.e. the sphere diameter or the distance between opposite corners for spherical particles or hexagonally shaped nanodiscs, respectively) was determined for each particle based on STEM images. At least 120 particles were measured to calculate the mean particle size and size distribution of each sample. IR spectra of the samples were recorded as pellets in potassium bromide with a FT-IR spectrometer Varian 660-IR (Agilent Technologies, USA). Raman spectra were acquired on a Senterra Raman microscope (Bruker Optics, Ettlingen, Germany). As excitation source a frequency doubled NdYAG-laser (λ = 532 nm) operated at 5 mW output power was used. Baseline correction with concave rubber band method (20 baseline points, 10 iterations) using Bruker OPUS software (version 7.8) was applied. Powder XRD measurements were performed with a PANalytical X'Pert Pro X-ray diffractometer employing Bragg-Brentano geometry with Cu-K_α radiation and a Ni filter. The diffractograms were recorded over a period lasting 8 h at room temperature. The reflections were compared to reference data reported in the Joint Committee of Powder Diffraction Standards (JCPDS) data base. Magnetization measurements (0–400 mT) were performed at 298 K with an alternating gradient magnetometer (AGM), MicroMag 2900 (Lake Shore Cryotronics, USA). The elemental composition of the nanodiscs was determined by ICP-OES with an Agilent 725 ICP-OES Spectrometer (Agilent Technologies, USA). For ICP-OES analysis, the samples were dissolved in concentrated hydrochloric acid.

3. Results and discussion

The Sc-doped barium hexaferrite nanodiscs were prepared *via* a hydrothermal synthetic procedure in which the precursors (i.e. $Ba(NO_3)_2$, $Fe(NO_3)_3{\cdot}9H_2O$ and $Sc(NO_3)_3{\cdot}H_2O$) were dissolved in water, precipitated with an excess of NaOH, and heated in a stainless-steel autoclave [19]. After reaching the target temperature of 160 °C, 210 °C, 260 °C, and 310 °C, accordingly, the autoclave was removed from the oven, the crude product collected and purified from $BaCO_3$ [18]. The nanodiscs were obtained as red-brownish solid. Fig. 1(a)-(d) displays the SEM images of the nanodics. Nanodiscs synthesized at 160 °C were small and 7 ± 4 nm and 8 ± 8 nm for molar Ba/Sc precursor ratios of 1:1 and 1:2, accordingly (Fig. 2). Furthermore, the particle morphology was influenced by the reaction temperature. In general, an increase in temperature led to an increase in size. Although this trend is apparent for both Ba/Sc precursor ratios, it seems to be more pronounced for the higher Sc-loading. Previously reported barium hexaferrite nanodiscs (i.e. obtained for a Ba/Sc precursor ratio of 2:1 at T = 240 °C) were 70 ± 38 nm in size. In our study, further increase of the Sc^{3+} dopant (Ba/Sc ratio of 1:1) and the increase of reaction temperature to 310 °C lead to nanodiscs with mean lateral dimensions of 59 ± 20 nm and thus to both smaller and more monodisperse particles [6]. The height of the nanodiscs (T = 310 °C) for a molar Ba/Sc precursor ratio of 1:1 was approximately 5 nm as estimated from the few nanodiscs in the STEM images which were aligned perpendicular to the grid.

Fig. 3 displays the TEM images of Sc-doped barium hexaferrite nanodiscs, which were obtained at 310 °C and an Ba/Sc precursor ratio of 1:1 (Fig. 3a) and 1:2 (Fig. 3c), respectively. The EDX line scans not only show that the nanodiscs consist of Ba, Sc and Fe but also that an increased amount of Sc^{3+} precursor also increased the amount of Sc^{3+} in the nanodiscs. These results are confirmed *via* ICP-OES. ICP-OES analysis showed that the Sc-doped barium hexaferrite nanodiscs contained Ba and Sc (Table S1, see SI). For a molar Ba/Sc precursor ratio of 1:1, the Ba/Sc ratio observed in the nanodiscs was similar to the ratio of the corresponding precursors used in their hydrothermal synthesis. In contrast, for a molar Ba/Sc precursor ratio of 1:2 (T = 160 °C and

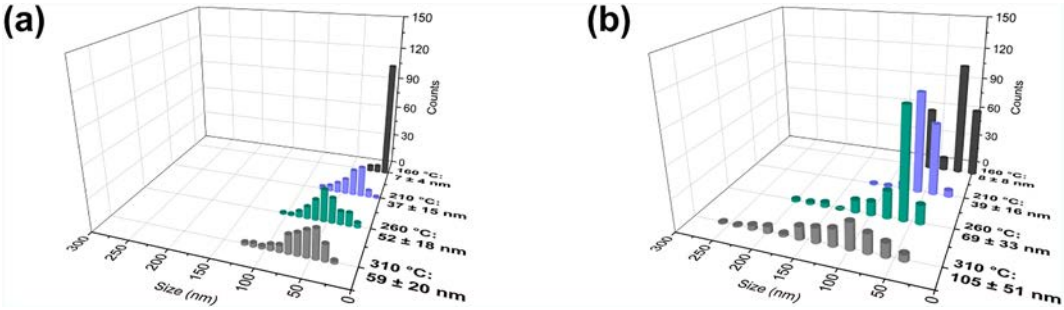

Fig. 2. Evolution of the lateral dimensions of nanodiscs obtained for a Ba/Sc precursor ratio of (a) 1:1 and (b) 1:2 at different reaction temperatures.

T = 210 °C), the ICP-OES analysis revealed nanodiscs which were enriched in Sc^{3+} with molar Ba/Sc ratio of the nanodiscs of 1:4.8. In this case, further increase of the reaction temperature yielded nanodiscs with a molar Ba/Sc ratio of 1:2.5.

Fig. 4 shows the results of XRD analysis of Sc-doped barium hexaferrite nanodiscs. All reflections observed for the Sc-doped barium hexaferrite nanodiscs could be assigned to the hexagonal $BaFe_{12}O_{19}$ phase, which is similar in lattice constant (JCPD 00–039-1433: 30.3° (110), 32.1° (107), 37.0° (203), 40.3° (205), 55.0° (217), 56.3° (304), 56.5° (20(11)), 63.0° (220), 67.3° (20(14)), 72.5° (317) (2Θ)) [20,21]. Nanodiscs obtained with a Ba/Sc precursor ratio of 1:1 were phase pure and exclusively revealed the reflections of the hexagonal $BaFe_{12}O_{19}$ phase. The XRD pattern of nanodiscs obtained with a Ba/Sc precursor ratio of 1:2, additionally revealed reflections of the $BaFe_4O_7$ phase (JCPD 01-070-1299) besides $BaFe_{12}O_{19}$ (Fig. 4b). In particular for the reflections at higher Bragg angles, a shift of the reflections to smaller Bragg angles (e.g. as illustrated for the (220) and (20(11)) reflections in Fig. 4a) was observed for Sc-doped barium hexaferrite nanodiscs as compared to the parent compound (JCPD 00-039-1433) indicating the insertion of the larger cation Sc^{3+} (0.745 Å) at Fe^{3+} sites (0.645 Å) in the barium hexaferrite lattice. Just recently, it was shown for polycrystalline $BaFe_{12-x}Sc_xO_{19}$ (for x = 2) that the Sc^{3+} ions were equally distributed among all of the Fe^{3+} sites [22]. Due to the anisotropic, platelet-like morphology of the particles, the XRD pattern revealed both broad and sharp reflections. As the height of the discs is small, reflections of planes perpendicular to the height of the discs were rather broad, while reflections of planes orientated perpendicular to the lateral dimension of the discs were rather sharp. The (*hk0*) reflections ((110) and (220)) were relatively sharp while (*hkl*) reflections (with $l \neq 0$) were much broader. These reflections were broad since the thickness of the nanodiscs (along the *c*-axis) was small. The thickness of the particles was estimated to 5 nm which corresponds to about two times the hexagonal unit cell along the c-direction (a = 0.5895 nm; c = 2.3215 nm). Consequently, nanodiscs obtained at 160 °C, where all

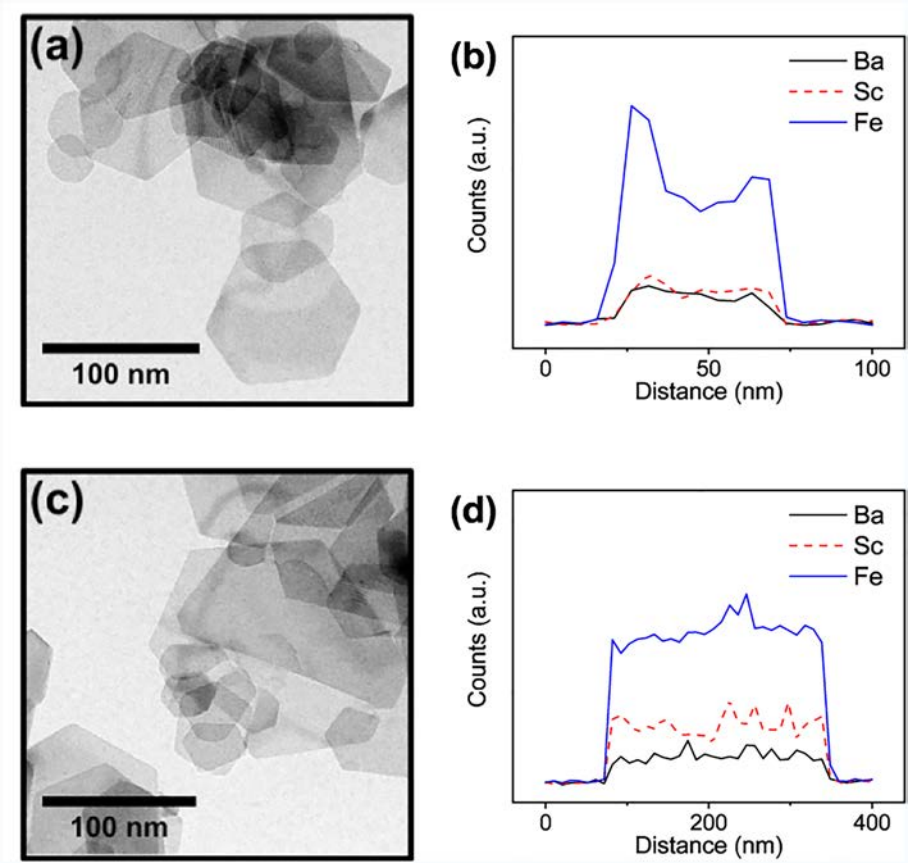

Fig. 3. TEM images of nanodiscs (T = 310 °C) with an initial ratio of Ba/Sc (a) 1:1 and (c) 1:2. (b) The EDX line scans of single nanodiscs (Ba/Sc ratio (b) 1:1 and (d) 1:2) reveal the presence of all three metal cations (Ba^{2+}, Sc^{3+}, and Fe^{3+}) in the nanodiscs.

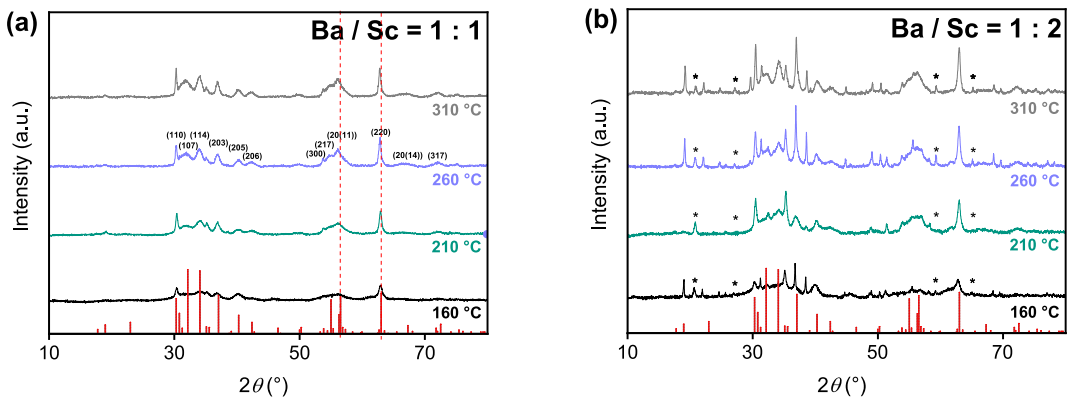

Fig. 4. XRD patterns of Sc-doped barium hexaferrite nanodiscs: Ba/Sc-ratio (a) 1:1 and (b) 1:2 for samples prepared at different reaction temperatures (T = 160 °C, 210 °C, 260 °C, and 310 °C). The reflections of the $BaFe_{12}O_{19}$ reference (JCPD 00-039-1433) are shown below. The reflections marked with* were assigned to the $BaFe_4O_7$ phase (JCPD 01-070-1299).

particle dimensions were small displayed only broad reflections. With increasing temperature (T ≥ 210 °C), (*hk0*) reflections (in particular the (110) and (220) peaks) increased in intensity and sharpened indicating further growth of the nanodiscs in lateral directions (Fig. 4a) [19]. Broadening of the reflections due to small nanoparticle sizes is a common phenomenon [14]. Recently, helical arrangements of the spins around the *c*-axis have been reported for Sc-doped barium hexaferrite (i.e. $BaFe_{10}Sc_2O_{19}$) by neutron diffraction measurements, giving rise to a longitudinal conical magnetic structure [22]. The magnetic easy axis aligned along the *c*-axis direction should be thus perpendicularly oriented to the plane of the nanodiscs. This is in good agreement with previous reports on similar particles [23].

The Raman spectra (Fig. 5a) show four bands for Sc-doped nanodiscs at around 673, 505, 400 and 320 cm^{-1}. The spectra look similar to undoped barium hexaferrite (undoped BHF) except for a slight change in the position of the Raman modes and the intensity of the bands observed. Sc^{3+} insertion at Fe^{3+} sites shifted the bands of undoped BHF to higher wave numbers (undoped BHF: 664, 497, 392, and 310 cm^{-1}). As a reference, undoped BHF was used, which was obtained using the same the reaction conditions but without adding scandium to the reaction mixture (T = 210 °C). The undoped BHF shows a decreased intensity of the band at 664 cm^{-1}, while the intensity of the bands at 392 and 310 cm^{-1} are increased with respect to the Sc-doped particles. After insertion of Sc^{3+} ions, all four bands observed in the Raman spectra were shifted to higher wavenumbers which could have been caused by doping of Sc^{3+} ions at Fe^{3+} sites [22,24]. Moreover, complementary FT-IR measurements were performed to detect structural changes in barium hexaferrite. Bands were observed in the IR spectra at 565 cm^{-1}, 425 cm^{-1} and 330 cm^{-1} which could be assigned to the vibrations of Fe–O bonds in undoped BHF (Fig. 5b).

In order to elucidate the magnetic properties, the nanodiscs were characterized *via* field-dependent magnetization curves with an AGM. Fig. 6a displays the room temperature magnetization curves for a Ba/Sc precursor ratio of 1:1. Apart from the reaction temperature, all reaction parameters of the hydrothermal synthesis were kept constant. In the investigated temperature range (i.e. 160–310 °C), $M_{0.4T}$ and H_c with 39.2 Am^2/kg and 57 mT, respectively, revealed a maximum for nanodiscs synthesized at 310 °C. When the amount of Sc^{3+} was further increased and thus the initial Ba/Sc molar precursor ratio Ba/Sc reduced to 1:2, particularly the samples received at high reaction temperatures (i.e. T = 260 °C, 310 °C) showed a reduced $M_{0.4T}$ and H_c and a kink in the hysteresis loop. Kinks in hysteresis loops have been previously observed for multiphase systems [25], but it may also result from particles with the same chemical composition but different sizes and thus different magnetization mechanisms. In these samples, some coffin-like particles were additionally detected besides the nanodiscs of hexagonal shape, while the amount of these particles decreased with lower temperature (see supporting information). This is in good agreement with the results of XRD analysis. In previous studies, Sc-doped barium hexaferrite particles with a $M_{0.8T}$ of 32.1 A m^2/kg (room temperature) and a H_c of 100 mT were obtained for a Ba/Sc precursor ratio of 2:1 [19]. In this study, the magnetization has been further enhanced with increase in reaction temperature (i.e. improving particle crystallinity) and Sc-dopant (Ba/Sc precursor ratio 1:1) while the further increase in Sc^{3+}

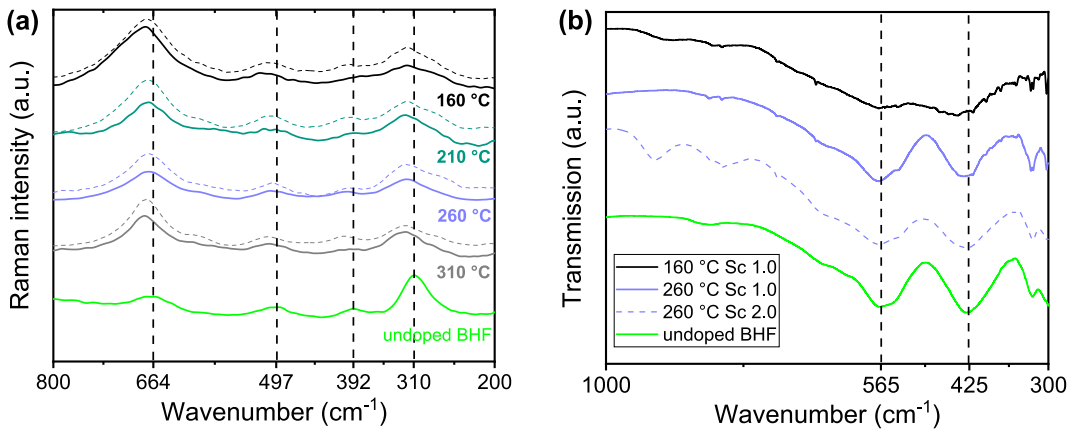

Fig. 5. (a) Raman spectra of nanodiscs for Ba/Sc ratio of 1:1 (solid lines) and 1:2 (dashed lines). (b) The IR spectra of Sc-doped barium hexaferrite nanodiscs reveal the characteristic bands of Fe–O vibrations. The bands of undoped barium hexaferrite (undoped BHF) at 565 cm^{-1} and 425 cm^{-1}, respectively, are marked.

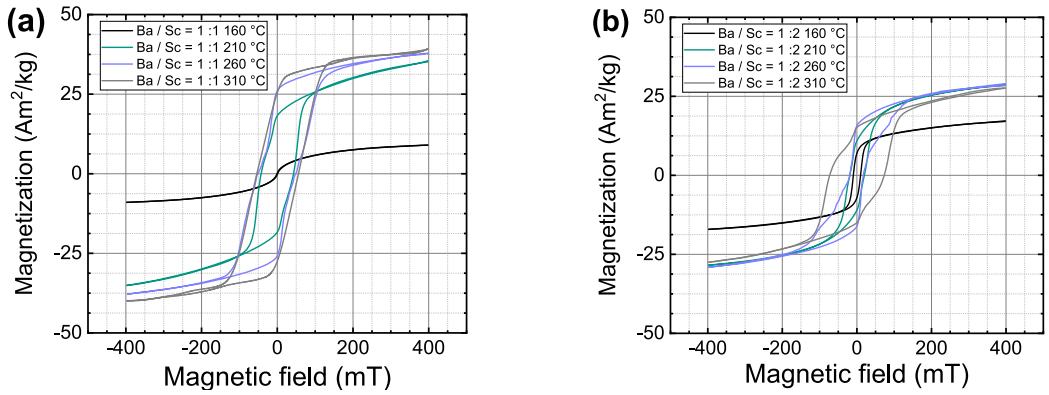

Fig. 6. (a)-(b) Field dependent magnetization curves for a Ba/Sc ratio of (a) 1:1 and (b) 1:2 obtained at room temperature.

seemed to induce the formation of multiphase samples with reduced M_s and H_c.

4. Conclusions

In summary, we have synthesized a set of magnetic Sc-doped barium hexaferrite nanodiscs *via* hydrothermal synthesis. The amount of Sc^{3+} in the reaction mixture and the reaction temperature significantly influenced the formation of the nanodiscs. In general, higher reaction temperatures led to bigger nanodiscs as a consequence of enhanced Ostwald ripening. At 160 °C, only small nanoparticles with a particle size of 7 ± 4 nm and irregular shape were obtained. With increase in reaction temperature, the shape of the nanodiscs became more regular and the particle size increased from 37 ± 15 nm (T = 210 °C), 52 ± 18 nm (T = 260 °C) to 59 ± 20 nm (T = 310 °C), respectively. The increase in the amount of Sc^{3+} precursor (Ba/Sc precursor ratio of Ba/Sc = 1:2 instead of 1:1) led to nanodiscs with larger lateral dimensions, while it also resulted in the formation of $BaFe_4O_7$ as a side product. Doping of the nanodiscs with Sc^{3+} led to nanodiscs with a room temperature $M_{0.4T}$ of 39.2 Am^2/kg (T = 310 °C, Ba/Sc precursor ratio 1:1) and a H_c of 57 mT. The hysteresis loop of the magnetization curves for samples prepared with a Ba/Sc precursor ratio of 1:2 showed a kink, which could indicate the presence of several magnetic phases and is in good agreement with the results of XRD analysis. Significant improvements of the intrinsic magnetic properties of M-type ferrites and/or modification of particle morphology may be achieved by the partial substitution of Ba^{2+} or Fe^{3+} ions, or both, by a plethora of divalent or trivalent cations (e.g. Ca^{2+}, Sr^{2+}, Al^{3+}, Ga^{3+} and others) and will be the subject of future investigations.

CRediT authorship contribution statement

Martin Hähsler: Investigation, Conceptualization. **Michael Zimmermann:** Formal analysis. **Stefan Heißler:** Formal analysis. **Silke Behrens:** Conceptualization, Funding acquisition.

Acknowledgements

We thank the German Science Foundation (DFG) for financial support of the projects BE2243/2 and BE 2243/3 within the Priority Program (SPP1681) “Field controlled particle matrix interactions: Synthesis, multiscale modeling and application of magnetic hybrid materials”.

References

[1] A.-H. Lu, E.L. Salabas, F. Schüth, Magnetic nanoparticles: synthesis, protection, functionalization, and application, Angew. Chem. Int. Ed. 46 (2007) 1222–1244.
[2] N.D. Burrows, A.M. Vartanian, N.S. Abadeer, E.M. Grzincic, L.M. Jacob, W. Lin, J. Li, J.M. Dennison, J.G. Hinman, C.J. Murphy, Anisotropic nanoparticles and anisotropic surface chemistry, J. Phys. Chem. Lett. 7 (2016) 632–641.
[3] A.-H. Lu, W. Schmidt, N. Matoussevitch, H. Bönnemann, B. Spliethoff, B. Tesche, E. Bill, W. Kiefer, F. Schüth, Nanoengineering of a magnetically separable hydrogenation catalyst, Angew. Chem. Int. Ed. 43 (2004) 4303–4306.
[4] S. Behrens, Preparation of functional magnetic nanocomposites and hybrid materials: recent progress and future directions, Nanoscale 3 (2011) 877–892.
[5] S.H. Chen, N.M. Amer, Observation of macroscopic collective behavior and new texture in magnetically doped liquid crystals, Phys. Rev. Lett. 51 (1983) 2298–2301.
[6] A. Mertelj, D. Lisjak, M. Drofenik, M. Čopič, Ferromagnetism in suspensions of magnetic platelets in liquid crystal, Nature 504 (2013) 237.
[7] K. Banerjee-Ghosh, O.B. Dor, F. Tassinari, E. Capua, S. Yochelis, A. Capua, S.-H. Yang, S.S.P. Parkin, S. Sarkar, L. Kronik, L.T. Baczewski, R. Naaman, Y. Paltiel, Separation of enantiomers by their enantiospecific interaction with achiral magnetic substrates, Science 360 (2018) 1331–1334.
[8] S. Behrens, I. Appel, Magnetic nanocomposites, Curr. Opin. Biotechnol. 39 (2016) 89–96.
[9] A. Gorschinski, G. Khelashvili, D. Schild, W. Habicht, R. Brand, M. Ghafari, H. Bonnemann, E. Dinjus, S. Behrens, A simple aminoalkyl siloxane-mediated route to functional magnetic metal nanoparticles and magnetic nanocomposites, J. Mater. Chem. 19 (2009) 8829–8838.
[10] S. Behrens, S. Essig, A facile procedure for magnetic fluids using room temperature ionic liquids, J. Mater. Chem. 22 (2012) 3811–3816.
[11] S. Essig, S. Behrens, Ionic liquids as size- and shape-regulating solvents for the synthesis of cobalt nanoparticles, Chem. Ing. Tech. 87 (2015) 1741–1747.
[12] B.T. Shirk, W.R. Buessem, Temperature dependence of Ms and K1 of BaFe12O19 and SrFe12O19 single crystals, J. Appl. Phys. 40 (1969) 1294–1296.
[13] X. Obradors, A. Collomb, M. Pernet, D. Samaras, J.C. Joubert, X-ray analysis of the structural and dynamic properties of BaFe12O19 hexagonal ferrite at room temperature, J. Solid State Chem. 56 (1985) 171–181.
[14] D. Primc, D. Makovec, D. Lisjak, M. Drofenik, Hydrothermal synthesis of ultrafine barium hexaferrite nanoparticles and the preparation of their stable suspensions, Nanotechnology 20 (2009) 315605.
[15] R. Müller, R. Hiergeist, H. Steinmetz, N. Ayoub, M. Fujisaki, W. Schüppel, Barium hexaferrite ferrofluids – preparation and physical properties, J. Magn. Magn. Mater. 201 (1999) 34–37.
[16] R. Müller, R. Hiergeist, W. Gawalek, A. Hoell, A. Wiedenmann, Magnetic and structural investigations on barium hexaferrite ferrofluids, J. Magn. Magn. Mater. 252 (2002) 43–45.
[17] R. Müller, R. Hergt, S. Dutz, M. Zeisberger, W. Gawalek, Nanocrystalline iron oxide and Ba ferrite particles in the superparamagnetism–ferromagnetism transition range with ferrofluid applications, J. Phys.: Condens. Matter 18 (2006) S2527–S2542.
[18] M. Drofenik, M. Kristl, A. Žnidaršič, D. Hanžel, D. Lisjak, Hydrothermal synthesis of Ba-hexaferrite nanoparticles, J. Am. Ceram. Soc. 90 (2007) 2057–2061.
[19] D. Lisjak, M. Drofenik, Chemical substitution—an alternative strategy for controlling the particle size of barium ferrite, Cryst. Growth Des. 12 (2012) 5174–5179.
[20] W.D. Townes, J.H. Fang, A.J. Perrotta, The crystal structure and refinement of ferrimagnetic barium ferrite, BaFe12O19*, Z. Kristallogr. 125 (1967) 437–449.
[21] W. Wong-Ng, H.F. McMurdie, B. Paretzkin, M.A. Kuchinski, A.L. Dragoo, Standard X-ray diffraction powder patterns of fourteen ceramic phases, Powder Diffr. 3 (1988) 246–254.
[22] S. Gupta, S.K. Upadhyay, V. Siruguri, V.G. Sathe, E.V. Sampathkumaran, Observation of magnetoelastic and magnetoelectric coupling in Sc doped BaFe12O19 due to spin-glass-like phase, J. Phys.: Condens. Matter 31 (2019) 295701.
[23] D. Lisjak, P. Jenuš, A. Mertelj, Influence of the morphology of ferrite nanoparticles on the directed assembly into magnetically anisotropic hierarchical structures, Langmuir 30 (2014) 6588–6595.
[24] W.Y. Zhao, P. Wei, X.Y. Wu, W. Wang, Q.J. Zhang, Lattice vibration characterization and magnetic properties of M-type barium hexaferrite with excessive iron, J. Appl. Phys. 103 (2008) 063902.
[25] H. Zeng, J. Li, J.P. Liu, Z.L. Wang, S. Sun, Exchange-coupled nanocomposite magnets by nanoparticle self-assembly, Nature 420 (2002) 395–398.